

# Assessment of wear on the cones of modular stainless steel Exeter hip stems

R. P. S. CHAPLIN\*, A. J. C. LEE, R. M. HOOPER

Department of Engineering, University of Exeter, Exeter, EX4 4QF, UK

E-mail: r.p.s.chaplin@exeter.ac.uk

The wear on the stem cones of retrieved Exeter Universal hip stems has been assessed using scanning electron microscopy (SEM), energy-dispersive X-ray analysis (EDX) and surface profilometry. The *in-service* life of these prosthetic stems varied, up to a maximum of 7 years. A combination of SEM, EDX and visual assessment indicates that the stem cones have not suffered from any corrosion. SEM scans indicate that damage to stem cones (excluding extraction and post-removal damage) can be categorised into insertion marks and fretting marks. In some cases there are signs of material being deposited on the cone surface. Surface profilometry suggests that the levels of debris generation at the cone/internal head interface are very low relative to those that are likely to be associated with head articulation against the acetabular cup. A total of 20 stem cones underwent SEM scans. From these, 10 subsequently have undergone surface profilometry along with the corresponding internal head surfaces. There is a good correlation between surface roughness measured by surface profilometry and the topography observed in the SEM images. The surface roughness of each stem cone is similar to that of the corresponding internal head surface.

© 2004 Kluwer Academic Publishers

## 1. Introduction

The majority of current commercial stems are modular, since they offer a number of advantages over single-piece stem systems. Modular systems function with the head achieving a push fit onto the stem cone, as indicated in Fig. 1. The head is placed onto the cone by the surgeon and then given a firm tap to locate it in position. A system of this type would be unsatisfactory, however, if it suffered from excessive corrosion or debris generation at the stem cone – internal head interface. Much work has been published on the generation of debris at the head and cup interface. Such work can be subdivided into *in vitro* simulations [1–4] and *in vivo* assessments or post-retrieval assessments [5–9]. It is generally acknowledged that the generation of such debris contributes to aseptic loosening of implants [10–14]. The inherent danger of any modular system is that a cone (neck taper or internal head) surface, that has been manufactured with insufficient control of dimensions, surface finish or material of construction, may undergo excess surface wear whilst *in-service* and that this wear will represent an additional source of debris (in addition to head/cup wear). Recently three papers have reported simulations that indicated that debris generation at the cone/internal head interface could be significant [15–17] for some systems, and Collier *et al.* [18] found evidence of corrosion at the internal head–stem interface for retrieved components

where a cobalt alloy head had been used with a titanium alloy stem. None of these publications relate to Orthinox<sup>®</sup> however, which is the steel used by Stryker Howmedica Osteonics for the stem and head of the Exeter total hip replacement (THR).

This report describes assessments made on the cones of 20 Universal Exeter hip stems and 10 of the corresponding internal head surfaces, post-retrieval. The stems were recovered from patients during revision operations at the Princess Elizabeth Orthopaedic Centre, Exeter. The medical history and clinical performance of these stems is shown in Table I. The stems in question are a mixture of the original modular Exeter hip stem, introduced by Howmedica in 1988 (Euro-cone), and the shorter cone modular stem (bearing the markings 5° 40' Ø14.3), introduced in 1991. The geometry of the two systems is shown in Fig. 1. The clinical performance of such stems has been reported by Williams *et al.* [19] and the survival rates for femoral aseptic loosening of 100% at 12 years indicate that, thus far, this type of stem can be regarded as being highly successful. This report concerns a study that aims to determine whether wear on any of the above-recovered stem cones was likely to have been significant or a contributing cause for revision. The study forms part of a more general study to develop methodology to study wear on any other stems that may be presented for assessment in the future.

\*Author to whom all correspondence should be addressed.

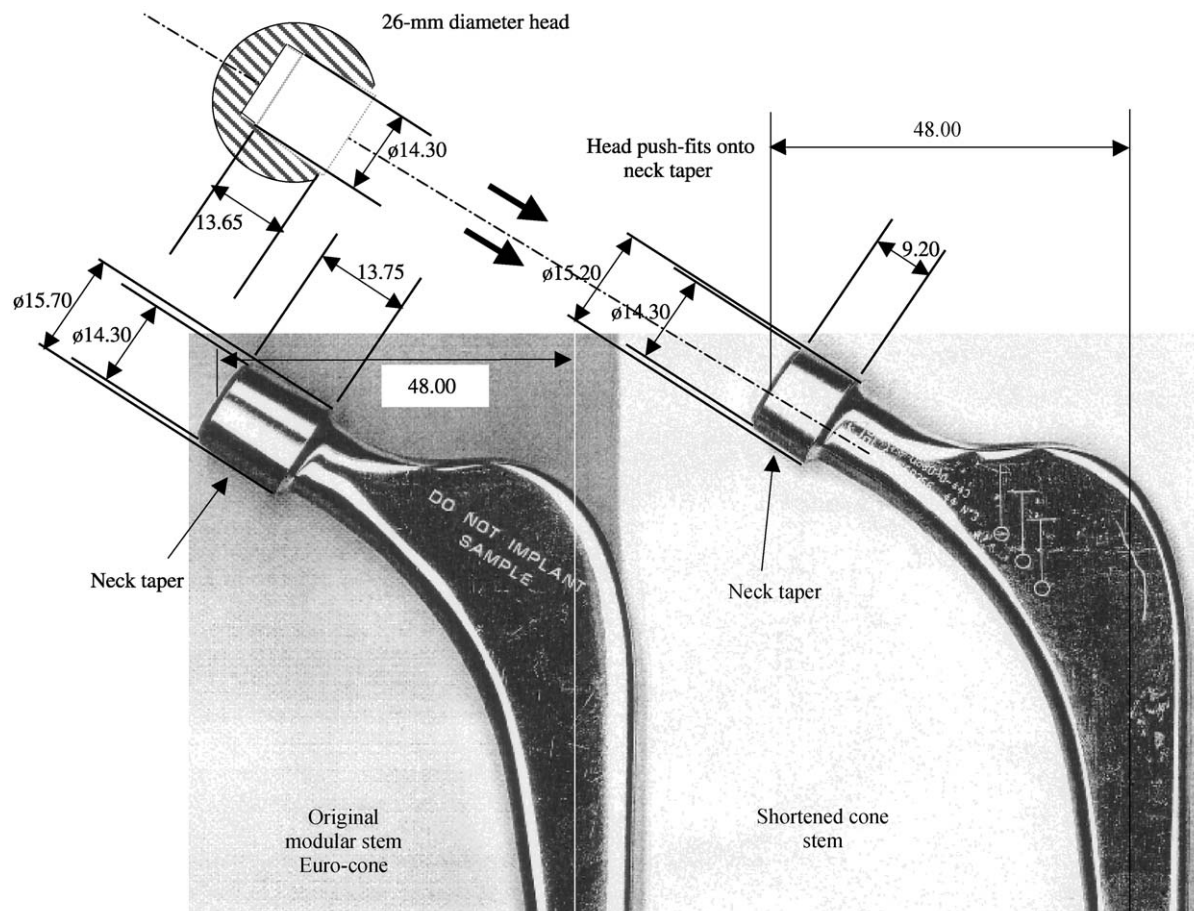


Figure 1 Geometry and dimensions of joint within modular stems (all dimensions in mm).

## 2. Experimental technique

### 2.1. Assessment of stem cones using scanning electron microscopy

Scanning electron microscopy (SEM) is a useful technique for assessing the surface condition of retrieved implants (or implants worn by simulation trials), and its use has recently been reported by several workers [20–22]. It can be used at high magnification to obtain

indications as to whether a surface has undergone chemical corrosion, and at lower magnifications to examine wear indicators that extend over several millimetres. The possibility of surface corrosion has been raised in a number of recent studies [18, 23–25], although none of these studied Orthinox<sup>®</sup>.

During the current study, in order to allow a view of all of the tapered surfaces, the stems were cut, using spark

TABLE I Clinical data supplied with stems

Number	In service life yr : m	Details
1	4 : 4	Periprosthetic fracture. Revision 15/4/99 (R)
2	5 : 2	Recurrent dislocation. 2nd Revision 23/3/2000 (L)
3	3 : 3	Infected THR – Loose cup – Revision 10/8/2000
4	Unknown	Recurrent dislocation due to part impingements. Revision 15/12/98
5	2 : 5	Socket graft, 2nd Revision loose cup and femur, 9/1/96 (L)
6	1 : 1	Recurrent dislocation. Revision 8/10/98 (R)
7	4 : 0	Well fixed grafted femur, loose socket. 29/10/98 (R)
8	6 : 6	Recurrent dislocation, sublux and sepsis. Socket eroded. 2nd Revision 24/9/98
9*	5 : 9	Revision of socket & femur grafted. Loose stem, 2nd Revision 8/9/98 (R)
10*	5 : 0	Loose (bipolar) 1/6/99
11	1 : 4	Revised cup, 2nd revision, stem well fixed 24/7/97 (R)
12	1 : 10	2nd revision. 13/8/98.
13	4 : 3	Both components loose. 2nd revision 9/7/98 (R)
14*	7 : 2	Well fixed stem, loose socket revised 3/6/99 (R)
15	1 : 2	2nd Revision 6/10/98 (L)
16	3 : 0	Socket revision, stem well fixed 3rd revision 18/3/99 (L)
17	5 : 0	Socket revision, stem well fixed 6/1/00 (L)
18	2 : 0	Recurrent dislocation cup & stem well fixed 13/1/95 (L)
19	2 : 0	Stem well fixed. 2nd revision of socket 27/7/99 (L)
20	3 : 0	Periprosthetic fracture revision 25/3/99 (L)

\*Original long tapered “Euro-Cone”. All others are short tapered cones.

In all cases both stem and cup were revised, even when the problem concerned only the cup.

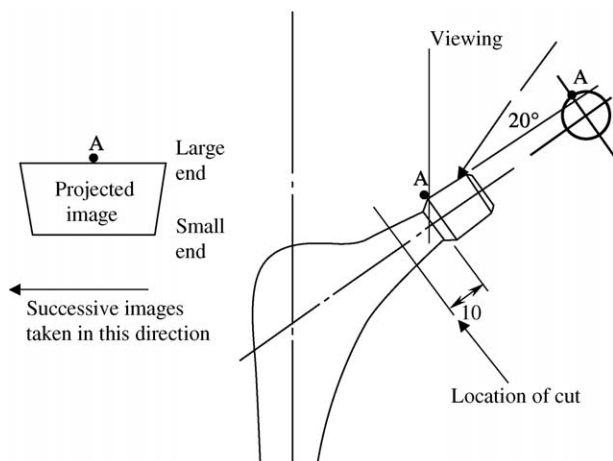


Figure 2 Presentation of the stem cone for SEM.

erosion, 10 mm below the taper (see Fig. 2). Care was taken during this (and the subsequent cleaning operation) to preserve the original surface features of the cones. Cleaning involved rinsing in a water/alcohol solvent followed by gentle drying with a lint-free cloth. Surfaces were protected during subsequent storage. Images generated using SEM were captured digitally.

The stems were mounted so as to give a 20° angle of incidence as shown in Fig. 2. The captured images therefore show the thin end of the cone taper at the bottom. The cones were rotated clockwise (when viewed

from the small end), so that successive images showed locations on the circumference displaced in an anti-clockwise direction (viewed from the small end). The datum (0°) for location around the circumference was the centre line of the proximal stem face, indicated in Fig. 2 using the letter A.

Where the SEM images appeared to show surface wear or damage, the wear was classified according to probable cause and graded on a 0, 1, 2, 3 system, as shown in Tables II and III. The majority of stems have suffered from some degree of random scratching, which is assumed to have occurred during the final stages of removal and/or during post-removal handling. The surface damage which is of interest – associated with possible *in vivo* debris generation – has been classified into (1) insertion, (2) surface roughness and/or deposition and (3) surface fretting. The way in which the *in-service* damage is distinguished from *post-service* damage is discussed in more detail further. Table II also shows that some cones appear to have more pronounced machining marks than others.

The grading system for apparent surface damage has been subdivided into wear that could be associated with the generation of debris *in vivo* and that which has occurred *post-service*. The former is the principal set of values shown in Table III. The bracketed values shown in Table III are the sum of *in vivo* wear and *ex vivo* damage – this is the value that should be related to surface profile

TABLE II Classification of types of surface damage

Stem number	Surface observation	Comments
1	I/P/M	Isolated locations around the stem
2	W/R	Moderate around most of the stem, heavy in some places
3	I	One location
	P/R/W	Moderate around most of the stem
4	R/W	Significant wear in one region only, signs of roughness across a slightly wider area
	I	At one location
5	W/P/R/M	Light to moderate only, covering part of the surface
6	W/P/M	Light across most of the cone
7	P/I	Heavy in some regions
	W/R	Moderate to heavy in several regions
8	M	Unusually pronounced at some locations
	R	Deposit around most of the wide end of the taper
9	W/R (M)	Visible around most and heavy across much of the surface, in some of the faint areas the fretting patterns appear to have been superimposed on heavy machining marks
	I	At one location
10	W/R (P/M)	Moderate in most places heavy in some
11	P	Heavy throughout
	W	Significant marking at one location only
12	W/R	Low marking at one location only
	M/P	Light in several places
13	No significant marks	(machining marks)
14	W/R/M	Low marking around most of the stem, moderate at a few locations. Faint fretting patterns blend into machine marking in places
15	I	At one location only
16	W/M	Light to moderate at a few locations only
17	W/M/R	Moderate to heavy in most places
18	W/R	Heavy marking at several isolated locations
	P	Moderate throughout
	M	Moderate in most places
19	P/M	Moderate at a few isolated locations
20	W/R (M/P)	Light to moderate around much of the stem, heavy in one place

W = fretting wear, R = roughness and/or deposition, I = insertion/extraction, M = machining, P = post operative.

Most stems show some degree of post-operative scratching.

TABLE III Classification of extent and location of surface wear

Location/°clockwise	0	72	144	216	288	
Wear*	<i>In vivo</i> wear only (total damage including <i>ex vivo</i> )					
Stem Core						
1	0.5 (1)	0 (0)	0 (0)	0 (0)	0 (0.5)	
2	2 (2)	3 (3)	3 (3)	1.5 (1.5)	3 (3)	
3	0 (0.5)	0.5 (1)	2 (2.5)	0 (2)	1 (1.5)	
4	0 (0)	2 (2)	1 (1)	0 (0)	0 (0)	
5	0 (0)	0 (0.5)	0 (0)	1.5 (1.5)	0.5 (0.5)	
6	0 (0)	1 (1)	0 (1)	0.5 (1)	0.5 (0.5)	
7	0 (0)	2 (2.5)	1.5 (3)	1.5 (2)	0 (1.5)	
8	0.5 (1)	1.5 (1.5)	1 (1.5)	1.5 (2)	1 (1.5)	Deposit on wide part of taper
9	1 (1)	2.5 (3)	2 (2)	1.5 (1.5)	2.5 (2.5)	
10	0 (0.5)	1.5 (1.5)	0 (1.5)	1.5 (1.5)	0 (0.5)	Deposit around 50° clockwise
11	0 (1)	0 (2)	0 (2)	0 (1.5)	0 (1.5)	
12	0 (0.5)	0.5 (1)	0 (1)	0 (0)	0.5 (0.5)	
13	0 (1)	0.5 (1.5)	0 (1)	0 (1)	0 (1)	Machining marks
14	0.5 (1)	2 (2)	0.5 (1)	1.5 (2)	(0.5) 1	
15	Big insertion mark at 261° clockwise – no other marks					
16	0 (0)	0 (0.5)	0 (0)	1 (1)	0 (0)	
17	1.5 (2)	3 (3)	1.5 (2)	2 (2.5)	1.5 (2)	
18	1 (1.5)	2.5 (3)	2 (1.5)	1.5 (2.5)	1 (2)	
19	0 (1)	0.5 (1)	0.5 (1.5)	0.5 (1)	0.5 (1)	
20	1 (1)	1 (1)	0 (0)	1.5 (1.5)	0.5 (0.5)	

\*Wear values: (a) Non-bracketed values refer to damage from fretting, roughness/deposition, and insertion/extraction, i.e. *in vivo* damage that could be associated with the generation of debris. (b) Bracketed value refers to all surface damage, that is, the above wear plus damage from post-operative handling and machining.

Key when relating numbers to surface wear: 0 = none, 1 = light, 2 = moderate, 3 = heavy.

Original assessments were all made in whole numbers and applied to a particular location  $\pm 5^\circ$ . Wear values shown above apply to the given location

measurements. The degree of wear shown for each location is the average wear around that location  $\pm 30^\circ$ . Surface damage is graded according to the product of degree of damage and area covered. Thus level 2 damage at a location  $\pm 30^\circ$  could mean moderate signs of wear across most of that area or alternatively heavy wear intermittently across that area.

## 2.2. Assessment of stem cones using energy-dispersive X-ray analysis

From the set of cones originally tested using SEM, nine cones were examined using energy dispersive X-ray (EDX). On these cones, SEM had indicated the possibility of one or more of the following:

1. Heavy fretting
2. Corrosion
3. Deposition and/or differential charging
4. Pronounced insertion marks

For each stem cone that was tested, an analysis was made on an area that appeared to be affected and on an area that appeared free from damage, when assessed using SEM. Table IV gives a summary of the cones that were tested, why they were tested, figures showing relevant SEM images and the chemical analyses as suggested by the EDX results. The chemical analyses are interpretations of the EDX spectra, made using Oxford Instruments<sup>®</sup> ‘‘Inca’’ software. It was noted that the software generated values for carbon that were very sensitive to the assumed presence or absence of traces of elements such as Na, Cl or K. For example, the unmarked area of cone 2, is shown in Table IV to contain 2.27% C

with the software set to ignore traces of Na, Cl and K, but if the software is set to assume the presence of these, then values become  $< 0.05\%$  C and  $0.06\%$  Cl. This means that C levels shown in Table IV may be several percentage points higher, particularly where the software has interpreted that no Cl, Na or K is present.

## 2.3. Surface profilometry of stem cones and internal head surfaces

The surface topography of 10 cones, and the corresponding femoral head internal surfaces was studied using the Taylor Hobson ‘‘Talyscan 150’’. This unit is equipped with laser and stylus options. It was used both directly on metal surfaces and on ‘‘Silflow<sup>®</sup>’’ silicone rubber replicas of surfaces. It was found that the laser gave too much noise when measuring both of these; in each case the surface was too smooth and consequently generated reflections that blinded the sensors. Measurements were therefore performed using a stylus with a tip of radius  $2\ \mu\text{m}$ .

Surface readings were filtered using a  $0.8\ \text{mm}$  Gauss filter. Calibration of the unit was made against a number of reference specimens with  $S_a$  values ranging from  $0.51$  to  $6.1\ \mu\text{m}$ . The unit was then used to measure the rubber replicas of these reference specimens. The replicas were shown to be faithful reproductions – a replica of the  $6.1\text{-}\mu\text{m}$  specimen gave an  $S_a$  of  $6.2\ \mu\text{m}$  and a replica of the  $0.51\text{-}\mu\text{m}$  specimen gave an  $S_a$  of  $0.63\ \mu\text{m}$ . When measurements were made on cone surfaces and on replicas made from them, however, a large disparity was noted. For example, the  $S_a$  values calculated for stylus directly on the cone from stem 1 ranged from  $0.45$  to  $0.48\ \mu\text{m}$ ,

TABLE IV Summary of the cones, EDX and SEM results

	C	O	Si	K	Na	Cl	Cr	Mn	Fe	Ni	Nb	Mo	SEM image	Damage indicated by SEM image
Cone 1													Fig. 3	Insertion/ploughing
Unmarked area	—	0.4	0.6				0.1	22.7	6.0	63.0	7.1	< 0.1	0.2	
Inclusion on surface	9.0	3.1	0.4				0.1	31.8	2.3	31.7	3.3	16.3	2.0	
Inclusion within the trough	4.9	0.6	0.3				< 0.1	20.8	6.4	60.3	6.5	0.2	—	
Trough of insertion mark	4.8	1.1	0.6				< 0.1	21.7	4.6	60.4	6.7	—	0.2	
Cone 2													Fig. 6	Fretting/pitting
Unmarked area	2.3	1.7	0.4	0.2			—	20.7	4.1	61.2	9.2	0.1	2.3	
Marked area	7.5	1.2	0.6				0.6	19.7	3.7	57.4	8.9	0.3	0.4	
Cone 3													Fig. 11	Insertion/deposition
Unmarked	5.0	1.4	0.5				—	19.4	4.5	58.4	9.1	0.3	1.5	
Shadow (trough) on insertion mark	21.1	3.9	0.8				0.2	13.9	2.0	52.7	4.3	—	1.1	
Peak on insertion mark	7.8	1.8	0.5	< 0.1			—	18.5	2.6	60.2	6.9	0.1	1.7	
Cone 4													Fig. 7	Deposit
Unmarked	1.6	1.6	0.5				—	20.6	4.2	60.0	9.2	0.1	2.2	
On deposit	5.5	1.9	0.5	< 0.1			—	20.1	4.2	56.4	8.5	0.6	2.5	
Cone 8													Fig. 5	Deposit
Unmarked	3.0	0.7	0.5				—	20.8	3.9	59.3	9.3	0.5	2.0	
On deposit	44.1	12.1	0.8	0.2			0.2	9.8	1.8	25.7	3.7	—	1.5	
Cone 9													Fig. 12	Fretting/roughness
Unmarked area	1.4	1.0	0.6				—	21.8	4.4	58.6	10.2	—	2.0	
Fretted area – dark	3.3	1.3	0.5				—	21.1	3.4	57.7	9.4	0.9	2.3	
Fretted area – light	0.8	0.6	0.3				0.1	21.3	4.2	60.5	10.4	0.2	1.8	
Cone 10													Fig. 13	Deposit/differential charge
Unmarked area	3.2	0.8	0.4				—	19.2	4.5	60.3	8.9	0.8	1.9	
Stained area	50.3	15.2	0.1	1.0	0.5	0.5	7.4	1.4	19.2	2.5	0.1	2.0		
Stained area	49.5	14.8	0.2	0.7	0.6	0.4	7.6	1.4	20.4	2.7	0.1	1.7		
Cone 17													Fig. 14	Fretting/roughness
Fretted	3.1	0.9	0.4	0.1			—	20.6	4.1	58.8	9.9	—	2.3	
Cone 18													Fig. 15	Fretting/roughness
Fretted	4.0	1.3	0.3	0.1			—	20.4	3.8	58.6	9.5	0.2	1.8	
Expected analysis for Orthinox								20.5	3.3	60	9.5	0.5	2.3	

Values shown are percentage by weight. Results are from single analyses.

Typical area scanned: background readings, fretted or stained areas 0.5 mm<sup>2</sup>; troughs/insertion marks, 50 μm<sup>2</sup>; inclusions, 1 μm<sup>2</sup>.

whereas the  $S_a$  values gained from the silicone rubber replica of cone 1 ranged from 0.92 to 1.3 μm. By studying SEM images it was realised that many of the features found on the cone surfaces were too narrow to be properly read by the stylus directly. The stylus tip radius plus its 90° cone meant that a 10-μm-wide mark could only be measured to a depth of 4 μm and marks thinner than 2 μm could not be detected. In contrast to this, the silicone rubber claims to be able to faithfully reproduce marks less than 2 μm wide. For this reason the silicone rubber replicas were adopted as standard surfaces on which to make surface measurements – immeasurable troughs on the original surface become measurable peaks on the replica.

Four of the stem cones that were tested (from stems 1, 5, 12, 15) had been indicated by SEM to have experienced very low levels of wear. Four of the stem cones that were tested (from stems 2, 7, 9, 17) had been indicated by SEM to have experienced very high levels of wear. Stem cones 3 and 8 were also tested – the former had apparently experienced an intermediate level of wear and had one pronounced insertion mark on the surface, the latter had a pronounced stain around the wide end of the taper. The surface profiles of all the corresponding internal head tapers were also measured, again via measurements made on rubber replicas.

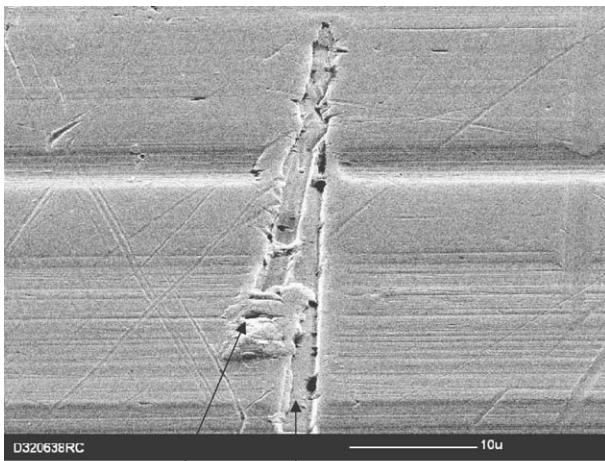
### 3. Results

#### 3.1. SEM images

##### 3.1.1. Head-cone insertion/extraction damage

Fig. 3 is an example of surface damage that has arisen during insertion of the head onto the cone and later by extraction of the head from the cone. It is believed that a hard third body has been present, the right hand of the two marks has been made during insertion and the left hand mark during extraction. Fig. 4 also shows an insertion/extraction mark – this time the damage has been caused by a relatively soft asperity or third body. Marks on the cones are thought to be due to head insertion or extraction if they run in the direction of the taper for 1 mm or more. There is likely to be evidence of ploughing or smearing of metal. The stems that show signs of this type of damage (denoted by the letter I in Table II) are stem numbers 1, 3, 4, 7 and to a lesser extent 9, 12 and 13.

The extraction of a head from a cone should be distinguished from the extraction of a stem from a patient. Both can cause what is referred to as “extraction damage” and neither will be directly associated with *in vivo* debris generation. The extraction of the head from the cone is closely associated with “insertion damage” however, which can lead to *in vivo* debris generation.



Extraction mark  
Insertion mark

Figure 3 Insertion/extraction mark caused by the presence of a hard third body on stem cone 1.

### 3.1.2. Surface roughness and/or deposition

Figs. 5–7 are examples of surface roughness and/or deposition that have been encountered. The roughened surface may appear pitted or there may be a deposit that charges differentially under SEM. It would be expected that such areas would show traces of oxide under EDX if corrosion had occurred. All cones where SEM indicates possible pitting or deposition have been checked using EDX, these are the cones from stems 2, 4, 8, 9, 10 and 18.

### 3.1.3. Surface fretting

Figs. 8 and 9 are examples of what appears to be surface fretting [26]. Fretting is defined by Waterhouse [27] as the action of two surfaces having oscillatory relative motion of small amplitude. It can be associated with the production of debris, usually an oxide, and signs of pitting or wear scars. Marks such as those shown in these figures form a repeating pattern, frequently cover large parts of cone surfaces and are usually only present on cones that show pronounced machining marks. The pattern consists of a series of curves, usually 100 µm long, forming a shallow angle with the machining marks. Cones that show evidence of significant fretting from

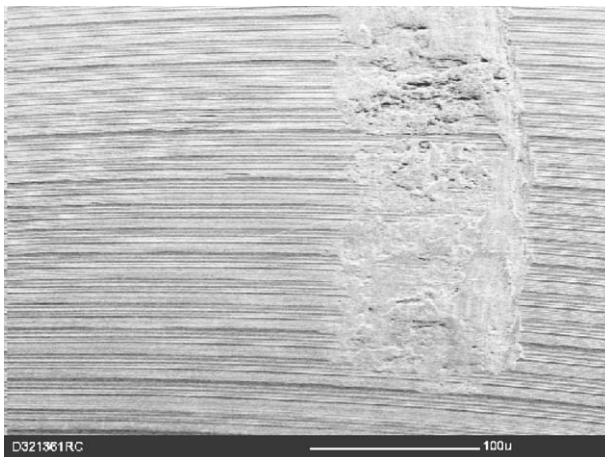


Figure 4 Insertion marks from soft third body or asperity on stem cone 4.

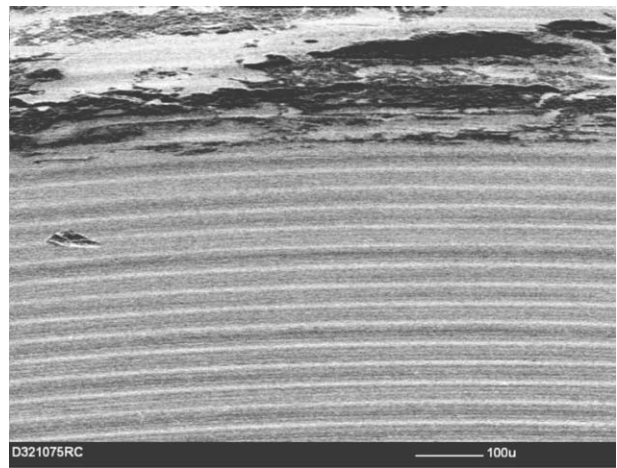


Figure 5 Surface deposit on stem cone 8.

SEM images are from stems 2, 7, 9, 10, 14, 17 and 18. The morphology of the damage is entirely consistent with that observed by Cooke [26] – both for clinical retrievals and laboratory experiments. Based on this comparison, it may be deduced that the marks have been caused by a repetitive relative motion between head and cone of approximately 50 µm, with the surface damage being superimposed upon machining marks.

On some stems where fretting patterns covered most of the surface, there was some suggestion of wear intensity

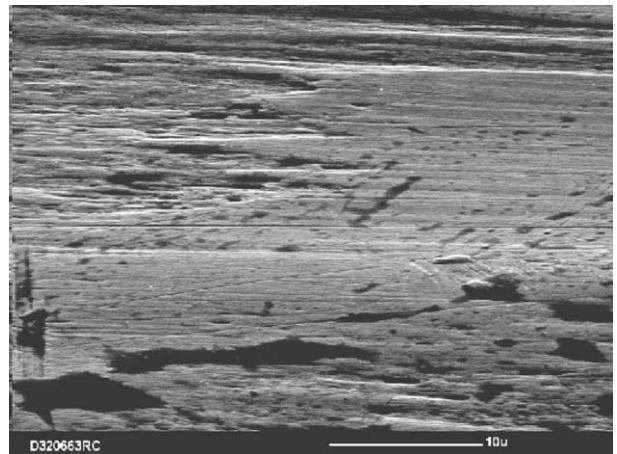


Figure 6 Heavy surface fretting leading to roughness on stem cone 2.

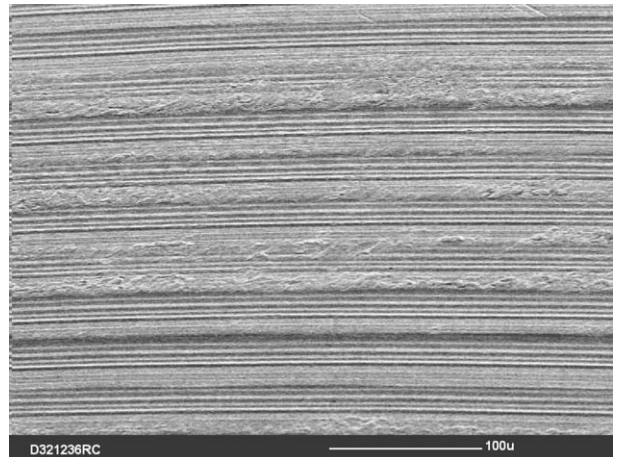


Figure 7 Surface deposit/roughness associated with fretting on stem cone 4.

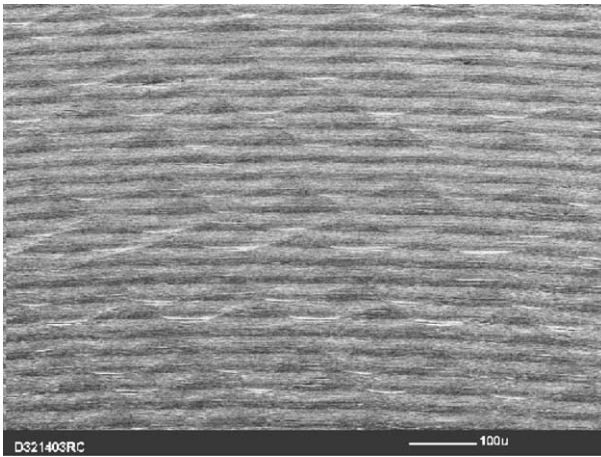


Figure 8 Fretting wear on stem cone 14.

being of a cyclic nature around the cone circumference. However, there was no systematic correlation between wear scar position and likely stress distribution. The form of the wear patterns does not suggest any link to procedures followed by surgeons, either during location or removal of the head. The total length of insertion/extraction marks shown in Figs. 3 and 4 can be several orders of magnitude greater than the wavelength of the patterns shown in Figs. 8 and 9.

#### 3.1.4. Machining marks

Fig. 10 is an example of what appears to be heavy machine marks.

### 3.2. EDX of cones

#### 3.2.1. Overview

Most elements were indicated as being present in the proportions appropriate to Orthinox<sup>®</sup> (Rex 734) stainless steel. Occasionally unexpectedly high levels of carbon were indicated – this could originate from body fluids transferred whilst *in vivo*, from handling *post-vivo* (e.g. hospital staff), or possibly even from the silicone rubber material. The presence of Na, Cl or K suggests a transfer of body fluids whilst *in vivo*. The presence of oxygen on analyses is to be expected if high levels of carbon have been measured. The corrosion of the stem is only

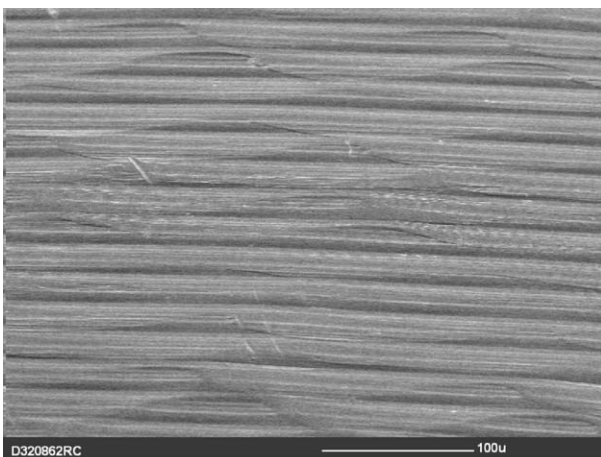


Figure 9 Fretting wear on stem cone 5.

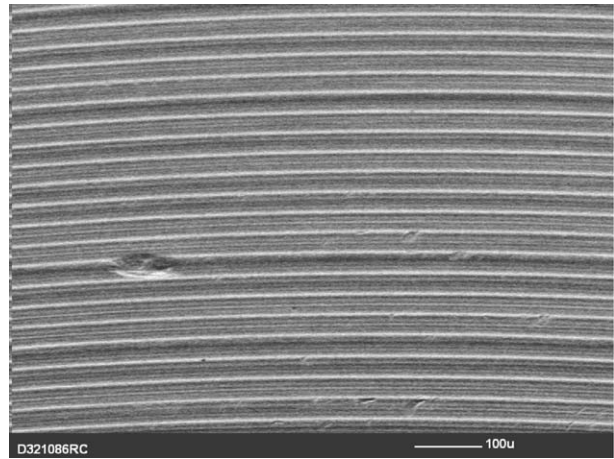


Figure 10 Heavy machine marking.

suggested by high levels of oxygen without the presence of C, Na, Cl or K. Si will be present at low levels within the metal, but there may also be a residue from silicone rubber replicas taken of the surface. The ‘inclusions’ referred to in Table IV are what appear to be individual particles of typically 1  $\mu\text{m}$ .

#### 3.2.2. Individual stems

Stem cone 1: SEM showed pronounced insertion marks thought to be caused by a hard third body. EDX analysis showed a particle with unusually high levels of Nb and C near to an insertion ‘trough’. Niobium is added to Orthinox<sup>®</sup> at levels of up to 0.8%. Its function is to stop chromium carbide precipitation at grain boundaries. This could result in hard niobium carbide particles being formed. Analysis of the insertion trough itself did not reveal anything significant.

Stem cone 2: SEM showed signs of heavy fretting and possible signs of surface corrosion. EDX analysis suggests slightly elevated oxygen levels, but not sufficient to suggest that corrosion has occurred.

Stem cone 3: SEM showed one area, shown in Fig. 11, where either a very wide insertion mark or else an area of deposition had been made. EDX suggests the presence of a carbon-based contaminant, but not corrosion.

Stem cone 4: SEM showed signs of deposition. EDX shows no evidence of corrosion.

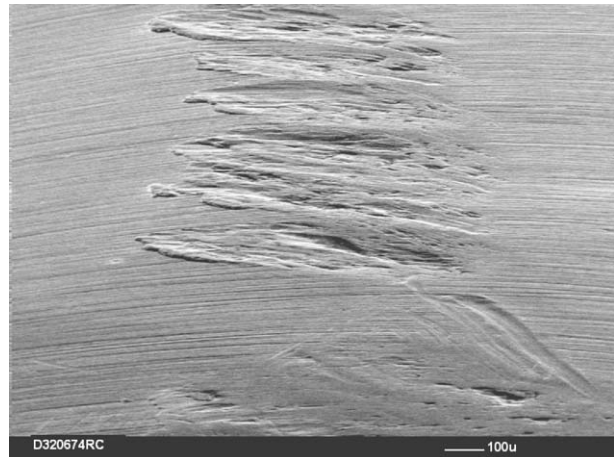


Figure 11 Deposit or possible insertion mark on stem cone 3.

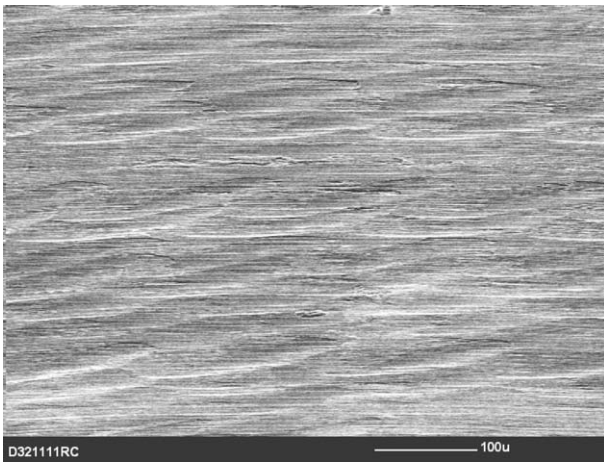


Figure 12 Signs of fretting on stem cone 9.

Stem cone 8: SEM showed a dark deposit running as a ring around the wide end of the cone taper. EDX showed that this was largely carbon and also contained other constituents of body fluids.

Stem cone 9: SEM showed signs of heavy fretting and possible signs of corrosion and deposition, shown in Fig. 12. EDX showed no significant compositional variations.

Stem cone 10: SEM showed an area that experienced differential charging under SEM, shown in Fig. 13. EDX indicated that the deposit was probably from human body fluids, being rich in Ca, Cl, K and C.

Stem cones 17 and 18: SEM indicated signs of heavy fretting and possible surface pitting, shown in Figs. 14 and 15. EDX showed no unusual compositional variations.

### 3.3. Surface profilometry

The Talyscan 150 and associated software can be used to generate surface images of moderate resolution (measurements taken every 5–10  $\mu\text{m}$ ), which can be tilted or rotated through any angle. Fig. 16 shows how the images produced using SEM and the Talyscan 150 can be matched together to form complimentary images. Because of its lower resolution, the Talyscan 150 cannot easily be used to measure specific features noted by SEM, for example, individual insertion marks.

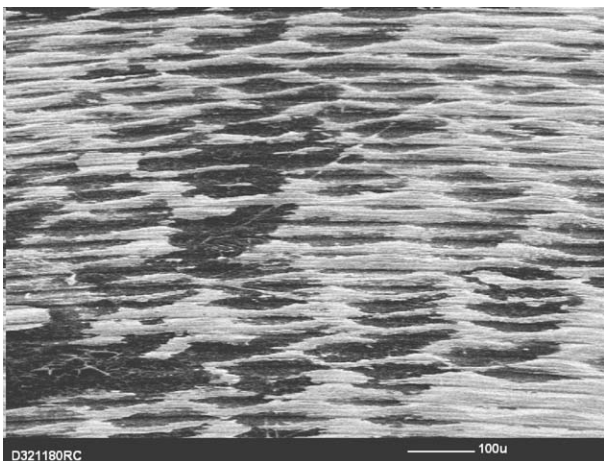


Figure 13 Differential charging shown on stem cone 10.

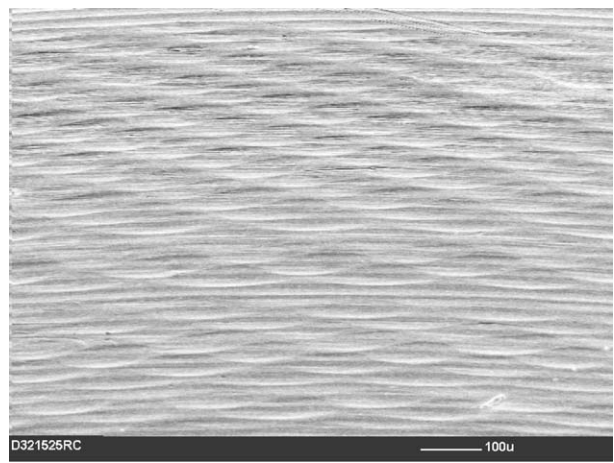


Figure 14 Signs of fretting on stem cone 17.

Instead each Talyscan run produces a surface map running the length of the taper and typically 80–90° around the circumference. In this way the total cone surface can be described by four or five such maps. The Talyscan software is then used to calculate parameters such as  $S_a$ ,  $S_p$  and  $S_v$  for each surface map.

When cone surfaces were divided into maps such as these, surface topography showed no area where the stem cone surface roughness, as defined by  $S_a$ , was in excess of 6.9  $\mu\text{m}$ . The roughness of internal head surfaces when mapped in this way was generally slightly less than the corresponding stem cone. The only two internal head surfaces that contained areas giving a surface roughness in excess of 3  $\mu\text{m}$  were from stems 7 and 9, whose stem cones were shown to be the roughest and third roughest of all cones tested. In this way there can be said to be a correspondence between stem cone and internal head roughness, although it should be noted that the internal head surface from stem 2 (second roughest stem taper) gave unexpectedly low surface roughness values.

The  $S_a$  values shown in Table V are generally less than 5  $\mu\text{m}$ . The exception to this is stem 7, which appears to have suffered excessive post-operative (*ex vivo*) scratching. In an ideal situation the  $S_a$  value for a given area could be used as an indicator as to whether *in vivo* wear has occurred at that location. In practice, damage arising from stem extraction and post-operative handling means that an SEM image for a given area must be

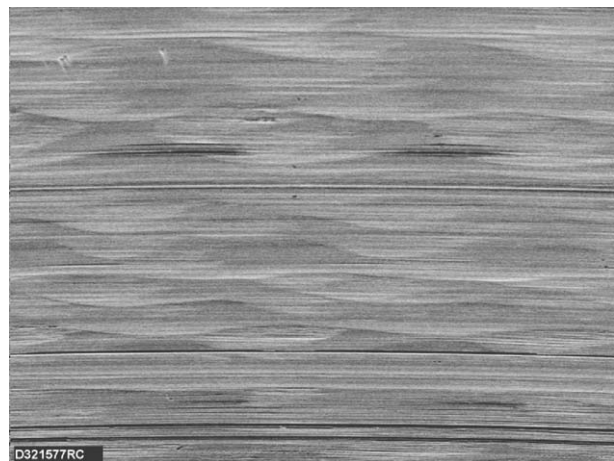


Figure 15 Signs of fretting on stem cone 18.



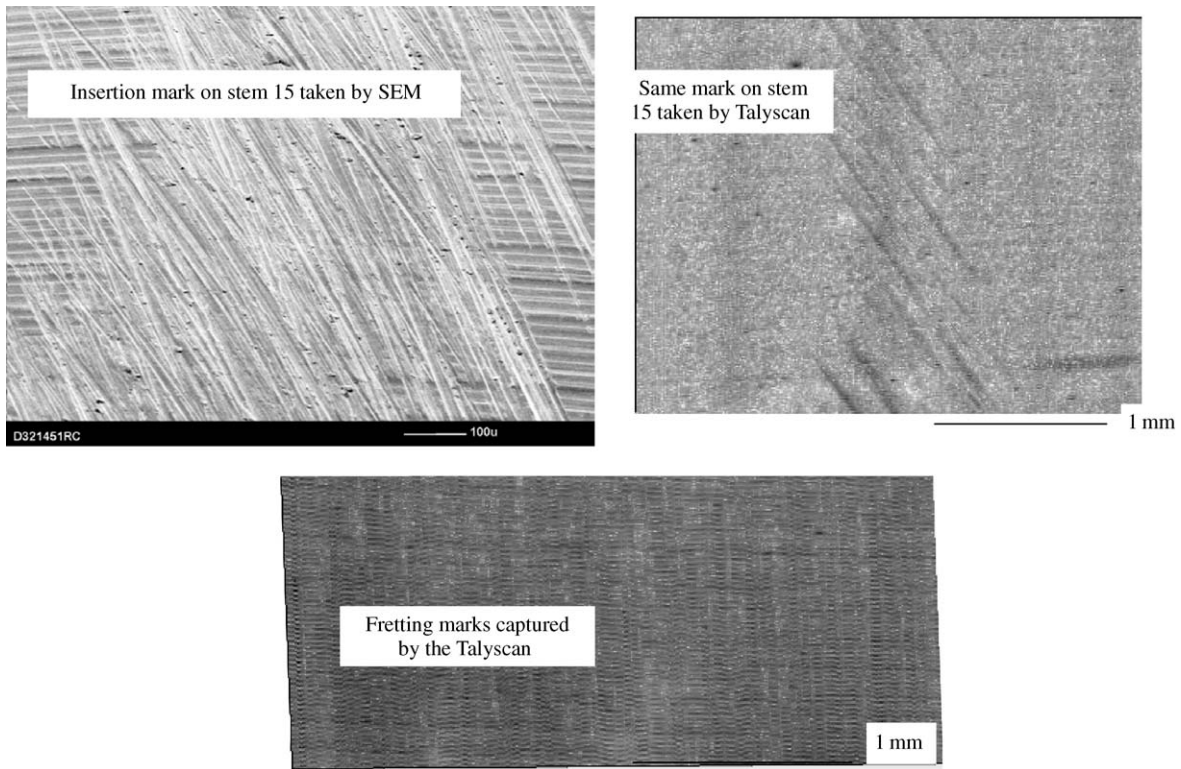


Figure 16 Comparison of images taken by SEM and Talyscan.

TABLE V Measurement of surface roughness and estimates

Stem number	Range of $S_a$ values/microns	Wear level estimated from SEM images
Virgin stem	0.58 to 1.10 (6 readings)	
Cone 1	0.92 to 1.25	0 to 1
Cone 2	4.22 at $-36^\circ$ to $+45^\circ$ 3.37 at $40^\circ$ to $90^\circ$ 1.70 to 1.76 $90^\circ$ to $184^\circ$ 4.95 at $195^\circ$ to $270^\circ$ 2.21 at $270^\circ$ to $345^\circ$	1.5 to 3
Cone 3	1.05 at $-45^\circ$ to $+45^\circ$ 1.21 to 2.8 $+45^\circ$ to $135^\circ$ 1.97 to 4.89 $+120^\circ$ to $+240^\circ$ 3.43 $+230^\circ$ to $310^\circ$	0 to 1 at $0^\circ \pm 80^\circ$ 1 to 2.5 at other locations
Cone 5	0.90 to 2.28	Mainly 0, but some worn areas (1.5 maximum)
Cone 7	3.92 $-55^\circ$ to $+45^\circ$ 2.41 $+55^\circ$ to $90^\circ$ 2.69 $+110^\circ$ to $+130^\circ$ 4.39 to 6.90 $+130^\circ$ to $230^\circ$ 1.37 $+235^\circ$ to $256^\circ$ 2.51 $+270^\circ$ to $315^\circ$	2.5 (0 to 1 from fretting, but stem is heavily scratched) 3 (high level of scratches) 2 0 to 1 from fretting, (1.5 to 2 with scratches)
Cone 8	1.04 to 2.62	0.5 to 1.5
Cone 9	1.44 $0^\circ \pm 30^\circ$ 1.83 $72^\circ \pm 30^\circ$ 4.07 $144^\circ \pm 30^\circ$ 4.53 $216^\circ \pm 30^\circ$ 2.30 $288^\circ \pm 30^\circ$	1 3 2 1.5 2.5
Cone 12	1.35 to 2.01	0 to 1
Cone 15	1.01 to 1.85 area around insert mark had $S_a = 1.3 \mu\text{m}$	0 to 1
Cone 17	1.60 to 2.44	Mostly 2, one peak at 3
Internal head 1	1.16 to 1.40	
Internal head 2	1.35 to 1.49	
Internal head 3	2.15 to 2.74	
Internal head 5	0.90 to 2.39	
Internal head 7	1.43 to 3.50	
Internal head 8	1.05 to 2.95	
Internal head 9	2.93 to 4.73	
Internal head 12	1.06 to 1.32	
Internal head 15	1.35 to 1.70	
Internal head 17	1.33 to 2.01	

studied, so that any surface disruption can be categorised according to cause. Overall there is a good correlation between the level of cone wear as indicated using SEM, and the surface roughness values indicated by the  $S_a$  and  $S_p$  values shown in Tables V and VI. Locations indicated by SEM to be free from wear typically give values for  $S_a$  of around  $1\ \mu\text{m}$  and have regularly occurring peaks of around  $4\ \mu\text{m}$ . Heavily worn areas have  $S_a$  values as high as  $5\ \mu\text{m}$  and regularly occurring peaks as high as  $10\ \mu\text{m}$ . A virgin stem that was tested had  $S_a$  values ranging from  $0.52$  to  $1.1\ \mu\text{m}$  and regular peaks of  $4.6\ \mu\text{m}$ .

Owing to the internal head surface measurements returning mostly low values for surface roughness, only limited conclusions could be drawn as to whether high surface roughness areas on stem cone and corresponding head surfaces were likely to have been aligned whilst *in-service*. The criteria that would need to be met before this was indicated were – (a) two or more areas existing on the stem cone that were significantly more rougher than the surrounding areas, (b) two or more areas existing on the internal head surface that were significantly more rougher than the surrounding areas, and (c) the relative locations of the rough areas being the same for both surfaces. The only two stems for which these criteria were met in full were stems 3 and 7.

Stem cones 3 and 8 had been selected for surface profilometry after notable features were seen on SEM images. Cone 3 showed one area with a low surface roughness; this corresponded to SEM images that suggested one area of low wear. The area that was indicated by SEM images to have an insertion mark was measured as having a high surface roughness. The SEM images for stem cone 8 had suggested a heavy dark deposit around the wide end of the taper. Surface profilometry failed completely to measure any surface disturbance in this area (although the background surface roughness was somewhat elevated). It may be concluded that what had been indicated by SEM images to be a significant deposit could better be described as a surface stain.

## 4. Discussion

### 4.1. The relative merits of SEM, EDX and surface profilometry in indicating surface damage

The high contrast of the SEM images may suggest a far heavier level of surface damage than actually exists,

particularly when viewed at high magnification. Results have shown that all surfaces indicated to be free of wear when analysed using SEM, have surface roughness values below  $2\ \mu\text{m}$  and will return standard compositions under EDX.

Energy-dispersive X-ray analysis is a useful tool for studying the composition of any particles found on the cone surface. It would be expected that oxygen levels would be far higher than those found on the stems tested if there were any significant corrosion. EDX is of no use in quantifying debris generation if the chemical analysis of that debris is similar to the cone surface.

Surface profilometry returns a range of roughness values that correspond well to SEM images. One factor that complicates any simple relationship between surface roughness and *in vivo* surface wear is the “pre-use” stem roughness, which is unknown for the stems tested and may not have been the same for all stem cones. This pre-use roughness depends primarily on the depth of any machining marks. Stem cones 1, 5, 12 and 15 appear to have no significant surface markings other than machining marking and each is classified from SEM images to have little or no wear. Owing to the variations in machining mark depth, average  $S_a$  values ranging from  $1.1$  to  $1.7\ \mu\text{m}$  are returned for these unworn stems. The average  $S_a$  value for a cone surface is the surface area weighted average of all measured values for that surface. The average  $S_a$  values returned for stems that appear to be significantly worn according to SEM images range from  $1.9$  to  $4.0\ \mu\text{m}$ .

### 4.2. Estimating the quantity of debris generated during the wear of cones

The surface area of the cone of a short taper modular Orthinox<sup>®</sup> stem that is in contact with the internal head whilst *in-service* is  $420\ \text{mm}^2$ . Most of the cones tested are of this type, although cones 9, 10 and 14 are the original longer taper type (Euro-cone), which has a cone surface area of  $640\ \text{mm}^2$ . The various alternative approaches to estimating level of debris generation based on surface topography measurements are described in the appendix and are referred to in Table VI.

Table VI shows, for each stem measured using the Talyscan:

1. A value for volume of material redistributed (assuming not removed) based on an average value for  $S_a$

TABLE VI Estimates of surface material loss or gain based on surface topography

Stem	Average $S_a$ ( $\mu\text{m}$ )	Average $S_p$ ( $\mu\text{m}$ )	Average $S_v$ ( $\mu\text{m}$ )	Material movement calculated by $S_a$ ( $\text{mm}^3$ )	Material removed calculated by $S_p$ ( $\text{mm}^3$ )	Material removed calculated by $S_v$ ( $\text{mm}^3$ )	Material removed calculated $S_v - S_p$ ( $\text{mm}^3$ )
1	1.09	3.72	3.60	0.06	-0.34	0.39	—
2	3.26	7.14	6.20	0.52	1.09	-0.70	—
3	2.56	5.51	4.67	0.37	0.41	-0.06	—
5	1.63	5.81	4.60	0.17	0.53	-0.03	—
7	3.96	5.13	5.11	0.66	0.24	-0.24	0.00
8	2.00	5.82	5.63	0.25	0.53	-0.46	—
9	2.83	6.21	6.97	0.43	0.70	-1.02	0.17
12	1.67	5.33	5.75	0.18	0.33	-0.51	0.09
15	1.26	4.33	5.78	0.10	-0.09	-0.52	0.34
17	1.89	5.80	6.62	0.23	0.53	-0.88	0.18

2. A value for volume of material removed based on an average value for  $S_p$  (with a wavelength of  $100\ \mu\text{m}$ ).
3. A value for volume of material removed based on an average value for  $S_v$  (with a wavelength of  $100\ \mu\text{m}$ ).
4. A value for volume material removed based on average  $S_v$  and  $S_p$  values as above, using the arithmetic mean of square and triangular profiles

The virgin (reference) cone has been measured as having the following values:  $S_a = 0.80\ \mu\text{m}$ ,  $S_p = 4.5\ \mu\text{m}$  and  $S_v = 4.5\ \mu\text{m}$ .

The calculation of volume of material removed based on  $S_p$  ( $100\ \mu\text{m}$ ) values assumes that material has been removed from less-frequently occurring peaks, that is, the height of the  $100\text{-}\mu\text{m}$  frequency peaks has not been eroded whilst *in vivo*. The calculation of volume of material removed based on  $S_v$  ( $100\ \mu\text{m}$ ) values assumes that no infilling has occurred between the frequently occurring valleys, that is, the depth of the  $100\text{-}\mu\text{m}$  frequency troughs has not been diminished whilst *in vivo*. In both cases calculations then proceed by comparing  $S_p$  and  $S_v$  values of recovered stems to those of the reference cone.

The somewhat contradictory results shown in Table VI indicate the limitations of trying to use surface profilometry to predict the amount of debris removal. The key data that are missing are the surface profiles prior to use. It is reasonable to assume that the peak and trough heights will be approximately equal on any virgin cone. On this basis, interpretation of the data in Table VI suggests the following surface profile histories for each stem.

Cone 1 has neither gained nor lost material, but had less pronounced machining marks pre-use than our reference stem (or has become smoother whilst *in vivo*).

For cone 2, the high  $S_p$  ( $100\ \mu\text{m}$ ) value suggests a worst-case scenario (for debris generation) where the peak height has increased whilst *in vivo* from the initial reference cone value by reduction of the mean surface height, as shown in Fig. 18. This worst-case value for debris generation is shown in column 6 of Table VI. The high  $S_v$  value indicates that this is extremely unlikely, however, and the negative value generated by this, shown in column 7, effectively cancels out the value shown in column 6. It is much more likely that both peak and valley heights were originally greater than those of the reference cones, and/or that subsequently the peak heights have been increased and/or the valleys filled in whilst *in vivo* as illustrated in Fig. 17. The value shown in column 7 of Table VI suggests that it may even be possible that the surface has accumulated rather than lost material.

Cones 3 and 5 are similar to cone 2, in that the values shown in column 6 of Table VI are worst-case scenarios for material loss. The high  $S_v$  values that both have

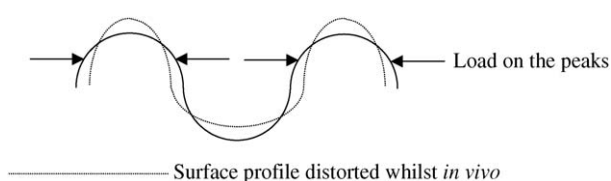


Figure 17 Showing a possible distortion of a surface whilst *in vivo*.

shown indicate that the pre-use values for  $S_p$  and  $S_v$  were probably greater than the reference values. The values for material loss shown in column 6 are thus likely to be significant overestimates.

Cones 7 and 8 are very unlikely to have either gained or lost material, the balance of peak and trough valley suggests that the surface has not been greatly disturbed. The pre-use peaks and troughs caused by machining were slightly greater than those of the reference stem. The worst-case scenario for material loss, which is very unlikely, is shown in column 6 of Table VI.

Cones 9, 12 and 17 are likely to have lost material from the surface by erosion of the  $100\text{-}\mu\text{m}$  frequency peaks. This is suggested because the  $S_p$  values are less than  $S_v$  values. As with other stems, the value for loss is unlikely to be as great as that shown in column 6 of Table VI, because the pre-use values for  $S_p$  and  $S_v$  for this stem were probably greater than those of our reference stem. The figures shown in column 8 are more likely values for material loss, although the theoretical maximum is actually slightly greater than that shown in column 6, if it assumed that peaks of  $100\text{-}\mu\text{m}$  frequency have been eroded.

For stem cone 15, worst case for material loss is shown in column 8 of Table VI. Material loss could only be greater than shown if the valley themselves have suffered erosion, which is very unlikely given the SEM images. It is likely that the level of material loss is less than shown in column 8, owing to the likelihood of some degree of valley infilling. It is likely that some material has been lost from this surface; this has not been signalled by SEM images since the material loss can best be described as a “polishing” effect.

### 4.3. The significance of debris generation

Combining estimates of worst possible levels of debris generation with the in-service lives indicated in Table I, the highest possible rate of debris generation is of the order of  $0.2\ \text{mm}^3\text{year}^{-1}$ , although the figure is likely to be much less. This maximum figure is equivalent to approximately  $1.6\ \text{mg}\ \text{year}^{-1}$ . Recently published papers indicate a range of debris generation; using a simulator Viceconti *et al.* [15] generated  $0.6\ \text{mg}\ \text{year}^{-1}$  at the tapered neck joint of a titanium alloy modular stem. Tipper *et al.* [1] simulated the movement of a variety of heads against a variety of cups. A ceramic head against a UHMWPE cup generated  $31\ \text{mm}^3/10^6$  cycles, metal on metal (MOM)  $1.23\ \text{mm}^3/10^6$  cycles, ceramic on ceramic (COC)  $0.05\ \text{mm}^3/10^6$  cycles, where  $10^6$  cycles was taken to be representative of one year’s use. Tipper *et al.* [2] produced wear of up to  $1.74\ \text{mm}^3/10^6$  cycles from COC with a microseparation during the load cycle. Stewart *et al.* [3] produced up to  $4\ \text{mm}^3/10^6$  cycles for COC in similar experiments. Goldsmith *et al.* [4] used a hip joint simulator and produced  $0.45\ \text{mm}^3/10^6$  long-term MOM wear, using a CoCrMo alloy. The initial wear rates were higher. The same simulator produced up to  $180\ \text{mm}^3\ \text{year}^{-1}$  for metal of polyethylene. Sieber *et al.* [5] retrieved 118 Metasul implants and found an initial MOM wear rate of  $25\ \mu\text{m}\ \text{year}^{-1}$ , falling to  $5\ \mu\text{m}$  after the first year. This

corresponds to approximately  $7.7$  and  $1.54 \text{ mm}^3 \text{ year}^{-1}$  respectively, which is described as approximately 1/60th of metal on plastic articulation. Emerson *et al.* [6] found wear levels within retrieved polyethylene cups to be  $190 \mu\text{m year}^{-1}$  from metal heads. Urban *et al.* [7] retrieved sockets with polyethylene wear from ceramic heads at  $28 \text{ mm}^3 \text{ year}^{-1}$ .

Recent studies [10–12, 14, 15] have concluded that adverse reactions to debris within the body depend upon the material and particle size as well as the total volume; titanium and polyethylene have both been cited as strongly contributing to osteolysis. Nevertheless, the estimates given in this paper for debris generation at the neck/head interface of Exeter Universal stems are an order of magnitude below those generated by MOM head/cup articulation and two orders of magnitude below the lowest debris generation obtained when using polyethylene cups.

#### 4.4. Relating the condition of recovered stems to clinical history

On the basis of SEM and surface profilometry, eight of the 20 stems recovered showed possible signs of *in-service* wear. The mean in service life of these eight stems was 4 years and 4 months, and the mean *in-service* life for all 20 stems was 3 years and 6 months. Of these eight stems, five had *in-service* lives of 4 years or more.

The causes for revision can be broadly classified into periprosthetic fracture, recurrent dislocation and other causes such as loosening or infection. The generation of debris would not contribute to the first two causes, although a recurrent dislocation might possibly increase the rate of debris generation. Aseptic loosening or infection could be exacerbated by excessive debris generation, however. Neither of the fractured stems showed signs of wear on the tapers. Three of the four recurrent dislocations showed tapers with signs of wear.

There is clearly an insufficient number of stems to allow any firm conclusions to be drawn from the above. Two possible indications might be that the stem wear does increase with *in-service* life and that recurrent dislocation may exacerbate stem wear. With only three of the stems being of the original Euro-cone, there is clearly insufficient data to make any comparison between the original modular Exeter stem and its shorter-tapered replacement. It can be seen, however, that all three of the original Euro-cones had *in-service* lives of 5 years or more.

### 5. Summary and conclusions

A total of 20 stem cones from retrieved Exeter Universal femoral components (original and shorter cone design) have been examined using SEM. From these, nine have subsequently been examined using EDX and 10 have undergone surface profilometry. The corresponding internal head surfaces have also been examined using surface profilometry.

No correlation has been found to link clinical performance, length of time *in vivo* and apparent surface wear as indicated by SEM imaging, although all of the stems that were in-service for 5 years or more showed signs of fretting wear. Table III does suggest that the minimum surface fretting occurs at the  $0^\circ$  location, suggesting that there is a minimum movement between head and cone at this location. There is a good correlation between SEM images indicating surface disruption and surface roughness values measured using the Talyscan 150. Surface roughness values measured using the Talyscan 150 can, to some extent, be used to generate estimates of *in vivo* debris generation. This is limited by the possibilities that smooth surfaces have been polished whilst *in vivo* and that relatively rough surfaces include pronounced (pre-use) machining marks.

Scanning electron microscopy was found to be a useful, rapid way to establish not only approximate relative surface wear, but also the type of surface disruption. This could be categorised into pre-service (i.e. machining marks), in-service (i.e. fretting or insertion marks) and post-service marks. The location of any marks was also noted. The Talyscan 150 could produce surface maps similar in appearance to low-magnification low-resolution SEM images. The lower resolution of the Talyscan made it hard for it to map some of the individual features identified using SEM. The surface profile maps have the advantage of being viewable from different angles and directions, and the surface roughness can be quantified. Surface roughness was quantified using  $S_a$ ,  $S_p$  and  $S_v$  values. Surface areas indicated by SEM to be free from wear gave values for  $S_a$  of between  $1$  and  $2 \mu\text{m}$  and had regularly occurring peaks of around  $4 \mu\text{m}$ . Heavily worn areas had  $S_a$  values as high as  $5 \mu\text{m}$  and regularly occurring peaks as high as  $10 \mu\text{m}$ . A virgin stem that was tested had  $S_a$  values ranging from  $0.52$  to  $1.1 \mu\text{m}$  and regular peaks of  $4.6 \mu\text{m}$ .

Energy-dispersive X-ray analysis showed that there is no evidence of stem corrosion or extreme variation in metal composition. A high presence of carbon was noted on occasions, which could come from a wide range of possible sources. No inexplicable contamination has occurred. There is no evidence to suggest that any corrosion has occurred. These findings are in contrast to those drawn recently by Goldberg and Gilbert [24], who found evidence of corrosion in systems where heads were Co–Cr–Mo and stems cones were either Co–Cr–Mo or Ti–6Al–4V. In their study, SEM images showed corroded surfaces at relatively low magnifications, whereas the Orthinox<sup>®</sup> stem cones do not appear to be corroded, in most cases, even when viewed at  $\times 1800$  magnification. It should be noted that the Goldberg and Gilbert study was a simulation of *in vitro* corrosion. Harding *et al.* [28] found that serum cobalt and chromium ion levels were no higher in patients with modular implants compared to non-modular implants.

Although the surface profilometry measurements cannot be used to give absolute values for the quantity of debris generated whilst in-service, the measurements can be reasonably interpreted to give an order of magnitude for debris generation. The worst case is indicated as being not greater than  $0.2 \text{ mm}^3 \text{ year}^{-1}$ , in most cases the wear is likely to be considerably less

than this. On this basis it is not believed that any *in-service* wear on these cones is clinically significant. This conclusion is in concurrence with Middleton *et al.* [29] who found that the introduction of modularity to the Exeter hip system had not increased instances of stem loosening.

## Appendix

### Use of surface topography measurements to estimate debris generation

#### Using $S_a$

Values of  $S_a$  cannot be used directly to indicate the level of debris removal from the surface whilst *in vivo*. They can, however, be used to indicate the extent to which material has been redistributed.

If a cone surface changes from smoothness  $S_a = S_0 \mu\text{m}$  to a roughness  $S_a = S_1 \mu\text{m}$  whilst *in vivo*, with all displaced material remaining attached to the surface, then the volume of material displaced ( $\text{mm}^3$ ) per  $\text{mm}^2$  will be

$$(S_1 - S_0)/2000$$

for a surface area of  $420 \text{mm}^2$  will be

$$0.21(S_1 - S_0)$$

For example, if stem cone 2 had an  $S_a$  of  $1 \mu\text{m}$  before use and an average value of  $3 \mu\text{m}$  post-use, then this could represent a material redistribution of  $0.42 \text{mm}^3$  around the surface of the cone.

#### Using $S_p$ (values on recovered stems compared to a reference "pre-use" value)

The height of peaks above the mean surface level,  $S_p$ , may be used in the estimate of the reduction in the mean surface height. Thus

$$R = S_{p1} - S_{p0} + X_1$$

where  $S_{p1}$  is the post-service value for  $S_p$ ,  $S_{p0}$  is the virgin value of  $S_p$ ,  $R$  is the reduction in mean surface height (in  $\mu\text{m}$ ) and  $X_1$  is the reduction in height of the peaks (in  $\mu\text{m}$ ) whilst *in vivo*. This is illustrated in Fig. 18.

For a surface area of  $420 \text{mm}^2$ , the total material removed (in  $\text{mm}^3$ ) will be  $0.42R$ .

Given the natural waviness of a cone surface and the existence of asperities, the value for  $X_1$  will vary depending on what is defined as a peak, and could even take a negative value. For the fretting patterns seen on SEM images, the wavelength of regularly occurring peaks is around  $100 \mu\text{m}$ . Peaks defined on this scale will not necessarily have been reduced in height, and may even be deposits – hence the possibility of  $X_1$  taking a negative value. This would be true of the load bearing points of contact occurred less frequently than every  $100 \mu\text{m}$ . The selection of these "fretting peaks", when making surface roughness measurements, is made by selecting  $2 \text{mm}^2$  areas that contain only regularly occurring peaks, not isolated peaks. The criteria are that the peaks should occur approximately 20 times in a

$2 \text{mm}^2$  area. Although the resolution of Talyscan images is not as high as SEM images, Fig. 16 shows the fretting patterns as captured by the Talyscan measurements.

If values for  $S_p$  are measured using peaks that occur less frequently than  $100 \mu\text{m}$ , a larger value for  $S_p$  is returned. The less frequent the peak, the less easy it is to relate the peak to those occurring on a virgin stem and hence the less use the value of  $S_p$  in estimating whether the mean surface level has changed. In other words if virgin and post-use peaks that occur on a wavelength of  $100 \mu\text{m}$  are being compared, then  $X_1$ , which is essentially unknown, is likely to be relatively small. If, however, peaks occurring on a wavelength of  $\text{mm}$  are considered, then both the values for  $S_p$  and also values for  $X_1$  will be greater.

#### Using $S_v$ (values on recovered stems compared to a reference "pre-use" value)

It can be assumed that troughs (valleys) on cone surfaces will not be significantly eroded, and are more likely to be filled whilst *in vivo*.  $R$ , the reduction in mean surface height, can thus be expressed using values for  $S_v$

$$R = S_{v0} - S_{v1} - Y_1$$

where  $S_{v0}$  and  $S_{v1}$  are mean surface to trough distances for virgin and post-use cones, respectively and  $Y_1$  is the increase in valley height.

The same arguments as before can be applied to justify the avoidance of infrequently occurring valleys in favour of those that occur on a wavelength of around  $100 \mu\text{m}$ . Use of this method is illustrated in Fig. 19.

#### Using $S_v$ combined with $S_p$

Assuming that the  $S_v$  and  $S_p$  values will be equal before use, if the post-use values for  $S_p$  are significantly less than the post-use  $S_v$  values then this suggests the possibility that material has been eroded via removal from the  $100\text{-}\mu\text{m}$  peaks.

If  $S_p$  values on recovered stems are greater than the  $S_v$  values then the likely possibilities are either that material has been gained and used to fill in the valleys, or alternatively that the mean surface level has dropped as shown in Figs. 18 and 19. Since two contradictory outcomes are possible, it is not appropriate to generate any values for cases, where  $S_p$  values are greater than  $S_v$  values.

Thus if post-use  $S_v$  values, are greater than  $S_p$  values then it may be assumed that the  $100\text{-}\mu\text{m}$  peaks have been reduced in height by

$$S_v - S_p$$

The mean reduction (or increase if negative) in surface height can be calculated by

$$R = \frac{S_v - S_p}{2} \quad \text{for a square wave profile}$$

or

$$R = \frac{(S_v - S_p)^2}{2S_v} \quad \text{for a triangular wave profile}$$

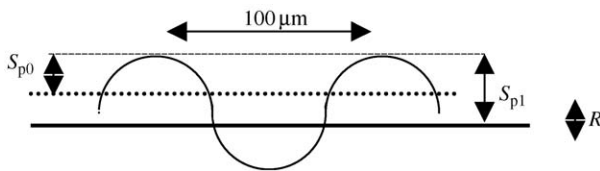


Figure 18 Illustration of how  $S_p$  values can be used to estimate reduction in mean surface height.

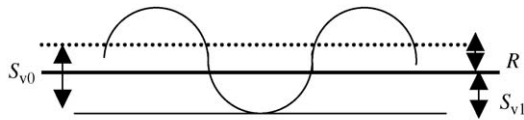


Figure 19 Illustration of how  $S_v$  values can be used to estimate reduction in mean surface height.

For Table VI the arithmetic mean of these two profiles has been used.

Assume that the mean surface position has been moved from . . . . . to ——— by the removal of peaks that occur less frequently than 100  $\mu\text{m}$ .

$$R = S_{p1} - S_{p0}$$

Where  $S_{p1}$  values for recovered stems are large this suggests the possibility that a reduction in surface height has occurred as shown above.

$$R = S_{v0} - S_{v1}$$

Where  $S_{v1}$  values for recovered stems are small, this suggests the possibility that a reduction in surface height has occurred as shown above.

## Acknowledgments

Acknowledgments are owed to Mr Graham Gie for recovering the implants and presenting them to the University of Exeter, and to Stryker Howmedica Osteonics, for their funding of the Research fellowship at the University of Exeter.

## References

1. J. L. TIPPER, P. J. FIRKINS, A. A. BESONG, P. S. M. BARBOUR, J. NEVELOS, M. H. STONE, E. INGHAM and J. FISHER, *Wear* **250–251** (2001) 120.
2. J. L. TIPPER, A. HATTON, J. E. NEVELOS, E. INGHAM, C. DOYLE, R. STREICHER, A. B. NEVELOS and J. FISHER, *Biomaterials* **23** (2002) 3441.
3. T. STEWART, J. TIPPER, R. STREICHER, E. INGHAM and J. FISHER, *J. Mater. Sci.: Mater. Med.* **12** (2001) 1053.
4. A. A. GOLDSMITH, D. DOWSON, G. H. ISAAC and J. G. LANCASTER, *Proc. Inst. Mech. Eng.* **214** (2000) 39.

5. H. P. SIEBER, C. B. RIEKER and P. KOTTIG, *J. Bone Joint Surg. [Br.]* **81** (1999) 46.
6. R. H. EMERSON, S. B. SANDERS, W. C. HEAD and L. HIGGINS, *J. Bone Joint Surg. [Am.]* **81** (1999) 1291.
7. J. A. URBAN, K. L. GARVIN, C. K. BOESE, L. BRYSON, D. R. PEDERSON, J. J. CALLAGHAN and R. K. MILLER, *ibid.* **83** (2001).
8. J. L. TIPPER, E. INGHAM, J. L. HAILEY, A. A. BESONG, J. FISHER, B. M. WROBLEWSKI and M. H. STONE, *J. Mater. Sci.: Mater. Med.* **11** (2000) 117.
9. R. M. HALL, P. SINEY, A. UNSWORTH and B. M. WROBLEWSKI, *Proc. Inst. Mech. Eng. Part H: J. Eng. Med.* **212** (1998) 321.
10. M. F. BASLE, G. BERTRAND, S. GUYETANT, D. CHAPPARD and M. LESOURD, *J. Biomed. Mater. Res.* **30** (1996) 157.
11. E. INGHAM and J. FISHER, *Proc. Inst. Mech. Eng. Part H: J. Eng. Med.* **214** (2000) 21.
12. R. M. URBAN, J. J. JACOBS, M. J. TOMLINSON, J. GAVRILOVIC, J. BLACK and M. PEOC'H, *J. Bone Joint Surg. Amer.* **82** (2000) 457.
13. A. S. SHANBHAG, W. MACAULEY, M. STEFANOVIC-RACIC and H. E. RUBASH, *J. Biomed. Mater. Res.* **41** (1998) 497.
14. Y. KADOYA, A. KOBAYASHI and H. OHASHI, *Acta. Orthop. Scand. Suppl.* **278** (1998) 1.
15. M. VICECONTI, M. BALEANI, S. SQUARZONI and A. TONI, *J. Biomed. Mater. Res.* **35** (1997) 207.
16. C. A. C. FLEMMING, S. A. BROWN and J. H. PAYER, *ASTM Spec. Tech. Publ.* **1173** (1994) 156.
17. S. K. BHAMBRI and L. N. GILBERTSON, *ibid.* **1173** (1994) 111.
18. J. P. COLLIER, V. A. SURPRENANT, R. E. JENSON and M. B. MAYOR, Transactions of the Annual Meeting of the Society for Biomaterials in conjunction with the International Biomaterials Symposium, Vol. 14, 1991, p. 292.
19. H. D. W. WILLIAMS, G. BROWNE, G. A. GIE, R. S. M. LING, A. J. TIMPERLEY and N. A. WENDOVER, *J. Bone Joint Surg. [Br.]* **84B** (2002) 324.
20. M. VICECONTI, O. RUGGERI, A. TONI and A. GIUNTI, *J. Biomed. Mater. Res.* **30** (1996) 181.
21. R. S. BOGGAN, J. E. LEMONS and E. D. RIGNEY, *J. Long Term Effects Med. Imp.* **4** (1994) 177.
22. M. SCHRAMM, D. C. WIRTZ, U. HOLZWARH and R. P. PITTO, *Biomed. Tech. Bio. Eng.* **45** (2000) 105.
23. J. L. GILBERT, C. A. BUCKLEY and J. J. JACOBS, *J. Biomed. Mater. Res.* **27** (1993) 1533.
24. J. R. GOLDBERG and J. L. GILBERT, *J. Biomed. Mater. Res. Part B: Appl. Biomater.* **64B** (2003) 78.
25. M. T. MANLEY and P. SEREKIAN, *Clin. Orthop.* **298** (1994) 137.
26. J. COOKE, PhD Thesis, University of Exeter, UK (1998).
27. R. B. WATERHOUSE, "Fretting Corrosion" (Pergamon Press, Hungary, 1972).
28. I. HARDING, A. BONOMO, R. CRAWFOR, V. PSYCHOYIOS, T. DELVES, D. MURRAY and P. MCLARDY-SMITH, *J. Arthroplasty* **17** (2002) 893.
29. R. G. MIDDLETON, D. W. HOWIE, K. COSTI and P. SHARPE, *Clin. Orthop.* **355** (1998) 47.

Received 15 July 2003

and accepted 26 February 2004